Diagn Interv Radiol 2008; 13:163-171

PICTORIAL ESSAY

Congenital anomalies of the aorta and vena cava: 16-detector-row CT imaging findings

Ömer Önbaş, Mecit Kantarcı, Mustafa Koplay, Haşim Olgun, Fatih Alper, Bülent Aydınlı, Hüseyin Zirek, Naci Ceviz

ABSTRACT

Cardiovascular specialists should be aware of the common types of congenital vascular anomalies and understand their implications for the patient's treatment and the likelihood of associated morbidity. Conventional angiography, the gold standard in vascular imaging, is an invasive and expensive method. Therefore, in recent years, less invasive techniques such as computed tomography angiography (CTA) and magnetic resonance angiography have become more widely used. Because of the recent advances in CT technology, multi-detector CTA has replaced conventional angiography in most clinical applications. Multi-detector CTA is a relatively new method and is very useful in the diagnosis and management of congenital aorta and vena cava anomalies. This study presents the radiological images of congenital anomalies of the aorta and vena cava, obtained through multi-detector CTA.

Key words: • *congenital abnormalities* • *aorta* • *vena cava* • *multi-detector CT angiography*

Congenital vascular anomalies are rare. However, physicians dealing with cardiovascular diseases must recognize these vascular anomalies and associated anatomic variations (1). Conventional angiography (CA) is considered the gold standard and is frequently used in vascular imaging. Nevertheless, because of the invasive nature and complications of CA, noninvasive methods such as magnetic resonance angiography (MRA) and computed tomography angiography (CTA) have been used with increasing frequency (2, 3).

Echocardiography is often the initial diagnostic method used in patients with suspected congenital cardiovascular disease. Although it provides sufficient evidence in many newborns, it is of limited use in some patients, particularly those with transpositions of the great arteries, pulmonary vein anomalies, and coronary artery anomalies. In addition, it may provide difficulty in interpretation of the images because of narrowed acoustic window in older patients. Magnetic resonance imaging (MRI) is an alternative that provides sufficient information with fast imaging through single-shot sequences; thus, MRI has been the primary choice in evaluating aortic and pulmonary anomalies. Nevertheless, its use is limited in severely ill or uncooperative patients, and it is contraindicated in patients with pacemakers. It is also time consuming and may require prolonged sedation of the patient (4). With the advent of multidetector computed tomography (MDCT) with multiplanar reformation (MPR) and three-dimensional (3D) volume rendering (VR) properties, the role of CT in evaluation of vascular anomalies, primarily of the aorta and vena cava, has increased. MDCT has modified the approach to vascular anomalies and raised the question of whether CA remains the gold standard in evaluation of vascular anomalies (5).

This study presents radiological images of congenital anomalies of the aorta and vena cava within a wide spectrum obtained through MDCT. In addition, literature review and sample figures of relevant cases are provided.

Technique

Perhaps the greatest advantage of MDCT—compared with conventional spiral CT—is that it is equipped with two or more series of multiple detectors along its longitudinal axis, and it can enlarge the x-ray collimation, resulting in faster table performance (6, 7). Furthermore, with the development of scanners that can complete the rotation of gantry at 360° in a very short time, the performance of MDCT has increased at a faster rate than CT (2, 3). The gantry rotational speed of MDCT is ≤0.4 s, minimizing artifact related to voluntary or non-voluntary patient motion, cardiac motions in pediatric patients, advanced age, and in trauma patients. Based on these properties of MDCT, a large volume can be scanned in a shorter time with thinner sections, higher spatial

From the Departments of Radiology (Ö.O. ✉ *oonbas@mynet.com*, M.Kantarcı, M.Koplay, F.A., H.Z.), Pediatric Cardiology (H.O., N.C.), and General Surgery (B.A.) Atatürk University School of Medicine, Erzurum, Turkey.

Received 15 February 2006; revision requested 17 April 2007; revision received 10 May 2007; accepted 13 May 2007.

resolution, and less contrast material (2, 3).

One of the main advantages of MDCT is its ability to perform CTA using lower than usual doses of contrast medium. The dose of contrast medium is based on its ability to reach maximum concentration within the vascular structure of concern, taking into account the age, weight, and cardiovascular status of a patient (2, 3). Proper delay time is adjusted, and a specific amount of contrast medium is administered at a specific time. Before the evaluation, approximately 10-15 mL of contrast material is given, and consecutive CT sections are obtained by test-bolus method to measure circulation of contrast medium within vascular structures at the time of highest concentration, when scanning can be achieved. This method, however, prolongs the time of evaluation and amount of contrast material. This issue can be minimized by systems that automatically determine the arrival of the contrast medium to the vascular structure and then start scanning based on this information (3).

In our study, 16-detector CT (Aquillon; Toshiba Medical Systems, Tokyo, Japan) was used to evaluate congenital anomalies of the aorta and vena cava. Patients with impaired renal function, allergy to contrast media, and advanced pulmonary disorders did not undergo CT evaluation. Before the evaluation, pediatric patients fasted for two hours and adult patients for four hours to prevent vomiting and its clinical complications. A venous line was opened through the antecubital vein before the patient was admitted to the evaluation room. Infants and young children were sedated for 2–10 minutes with chloral hydrate (oral 50–100 mg/kg) or pentobarbital sodium (i.v. 6 mg/kg) to minimize movement during imaging. The scans were performed in sections of 1–2.5 mm, reconstruction intervals of 1 mm, and a helical pitch of 1. Values for mAs for infants and young children were 50–80, and 80–140 in adults. Non-ionic contrast medium (2 mL/kg) was given with an automatic injector at a rate of 4 mL/s. Imaging was performed on axial plane after proper phase for the aorta and the vena cava was determined.

After the basic images of all the patients acquired on axial plane were evaluated in detail, using special computed software and MPR, maximum intensity projection (MIP), curved planar reformation (CPR), shaded surface display (SSD), and VR methods, images of 2 or 3 dimensions on different planes were developed. Based on these images, congenital anomalies of the aorta and vena cava and accompanying anatomic variations were clearly observed.

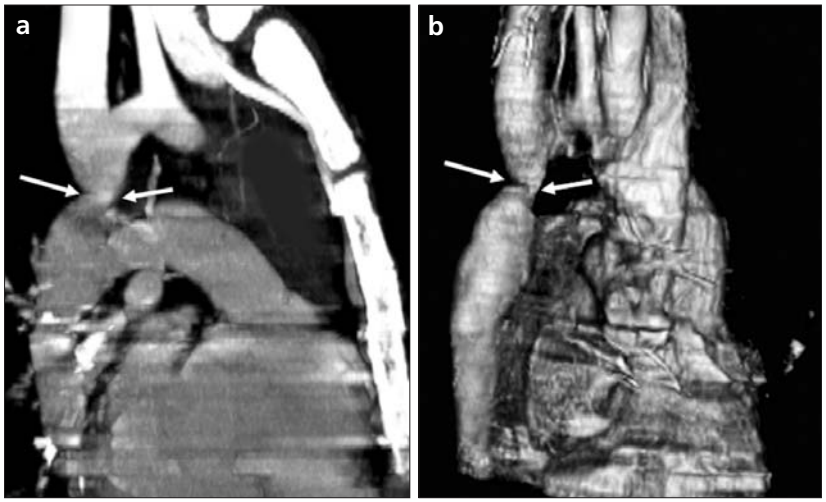

Figure 1. a, b. Aortic coarctation. On sagittal maximum intensity projection **(a)** and three-dimensional volume rendering **(b)** CT images of a 12-year-old patient, the coarcted segment is observed in the descending aorta *(arrows)*.

I. Aortic anomalies

Radiologic assessment of aortic anomalies is essential in planning surgical intervention. Echocardiography is diagnostic in aortic valve diseases; however, it has a limited use for an evaluation of aortic coarctation, aberrant vessel anatomy, and the ascending aorta. Visualization of congenital aortic arch anomalies is possible even in newborns (4).

I. a. Aortic coarctation

Coarctation is a congenital stenotic anomaly of the aortic lumen, typically located between the left subclavian artery and aortic isthmus. Infrequently, coarctation may also be detected at the level of subclavian artery or between the left carotid artery and subclavian artery (8–10).

Coarctation is seen in 8% to 10% of all the patients with congenital cardiac defect and is twice as common as other congenital cardiac defects. Bicuspid aortic valves are seen in 85% of patients with aortic coarctation (11). Collateral circulation is provided by internal mammarian, costocervical, and intercostal arteries; these enlarged collaterals cause the characteristic sign of rib notching on chest radiogram. These patients present findings of congestive heart failure, cardiomegaly, hypertension, weak femoral pulse, and differences of blood pressure between upper and lower extremities.

Aberrant right subclavian artery accompanied by coarctation has also been defined. Dilatation of aorta typically occurs in the segment distal to coarctation. Uniform stenosis of aortic arch (tubular hypoplasia) may be common in the newborn. Localized coarctation and tubular hypoplasia might coexist or occur separately (8, 12).

As imaging methods, chest radiography, echocardiography, and MRI provide important information. In patients with coarctation, MDCT with MPR and 3D imaging clearly show the area of stenosis and its length, poststenotic dilatation, collateral vessels, accompanying arch hypoplasia, aneurysm, and single or multiple layers of coarctation (Fig. 1).

1. b. Double aortic arch

Double aortic arch is a congenital anomaly characterized by persistence of the right and left embryonic arches; it is the most common cause of vascular ring (13, 14). Generally, one of the arches is dominant. The left carotid and subclavian arteries branch from the left arch, and the right carotid and subclavian arteries branch from the right arch. The right arch typically passes behind the esophagus, joins the left arch,

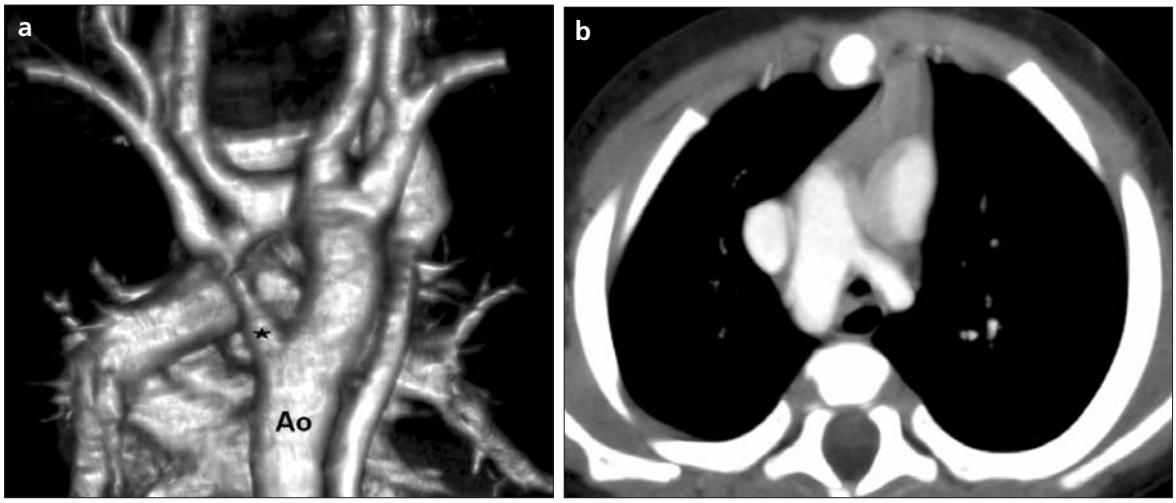

Figure 2. a, b. Double aortic arch. On three-dimensional volume rendering CT image **(a)** of a 10-month-old patient, double arch is observed on a posterior view (Ao, Aorta; star, rudimentary arch). On the axial CT section **(b)**, the aortic arch splits into two and surrounds the trachea and esophagus.

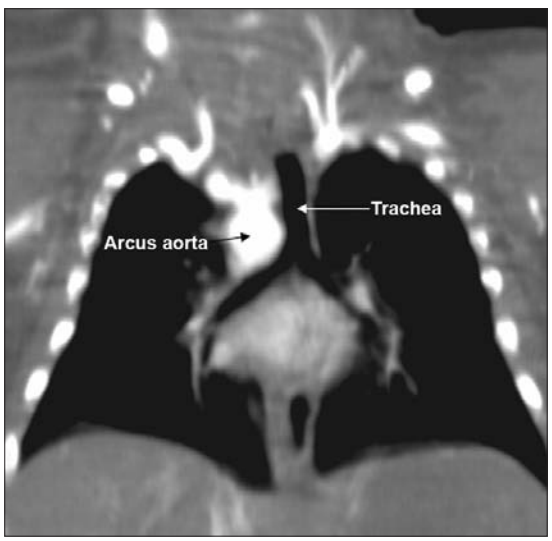

Figure 3. Right aortic arch. On coronal reformatted CT image of a 4-month-old patient, the aortic arch is located on the right of the trachea.

and forms the aorta coursing down on the left. It forms a double aortic arch ring along with the ascending aorta and may compress the trachea and the esophagus. Symptoms typically present at an early age and are caused by compression of the trachea or esophagus (14, 15). The ductus arteriosus usually connects with the left arch. However, it may also arise from the right arch or from both sides. Shorter ductus arteriosus may cause increased compression because it exerts a posterior pull on the pulmonary artery and an anterior pull on the aorta.

Diagnostic methods such as chest radiography, barium study, echocardiography, CT, and MRA may be used. The sectional images obtained through MDCT, particularly axial, coronal, and 3D imaging, are highly useful. The axial image at the level of thoracic inlet shows four aortic branches (2 carotid and 2 subclavian) originating symmetrically; two arches surrounding the trachea and esophagus and causing the stenosis are also seen. Three-dimensional images are valuable in displaying the relation of the arch anatomy to the esophagus (Fig. 2).

I. c. Right aortic arch

In this anomaly, the aortic arch is located on the right main bronchial trunk and on the right of the trachea. The vessels originating from the arch are a mirror image of normal structures, and the structure completing the ring is the ductus ligament or the ductus located on the left. It is the second most common cause of vascular ring and embryologically, it is formed due to persistence of the fourth right aortic arch. The symptoms of the right aortic arch are due to the compression on the trachea and sometimes on the esophagus (15, 16).

In the anomaly of aberrant left subclavian artery branching off the right aortic arch, the first trunk branching off the arch is the left common carotid artery, the second trunk is the right common carotid artery, the third trunk is the right subclavian artery, and the last trunk is the left subclavian artery. The left subclavian artery, while passing posterior to the aorta and extending to the left arm, may cause compression on the esophagus and dysphagia. In this anomaly, the ductus arteriosus is usually on the left. The remains of the left dorsal aortic root are detected as diverticula (Kommerell diverticula) in the origin of the left subclavian artery. The posterior of the arterial ring is composed of aberrant left subclavian artery and Kommerell diverticula; the anterior, of the ascending aorta and pulmonary artery; the right side, of aortic arch, and the left side, of ligamentum arteriosum (7).

Imaging methods are chest radiography, barium study, echocardiography, CT, and MRI. Through MDCT, the segments of the arch can be clearly shown on the axial images, and compression on the trachea on the coronal/sagittal images (Fig. 3).

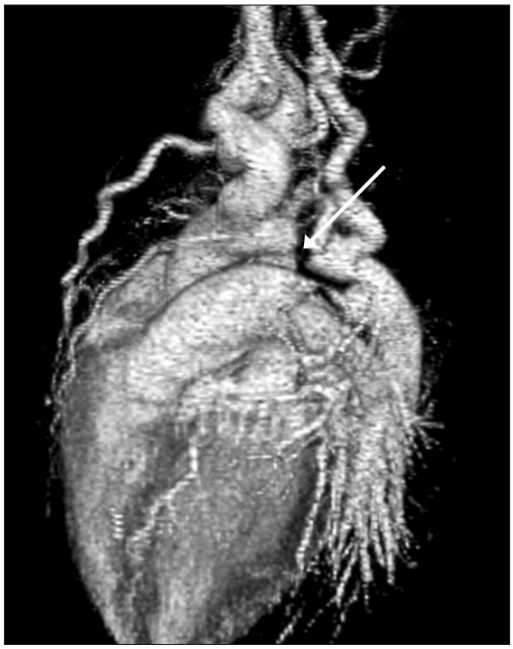

Figure 4. Interrupted aortic arch. On three-dimensional volume rendering CT image of a 20-day-old infant, interrupted aortic arch is shown through a left oblique view *(arrow)*.

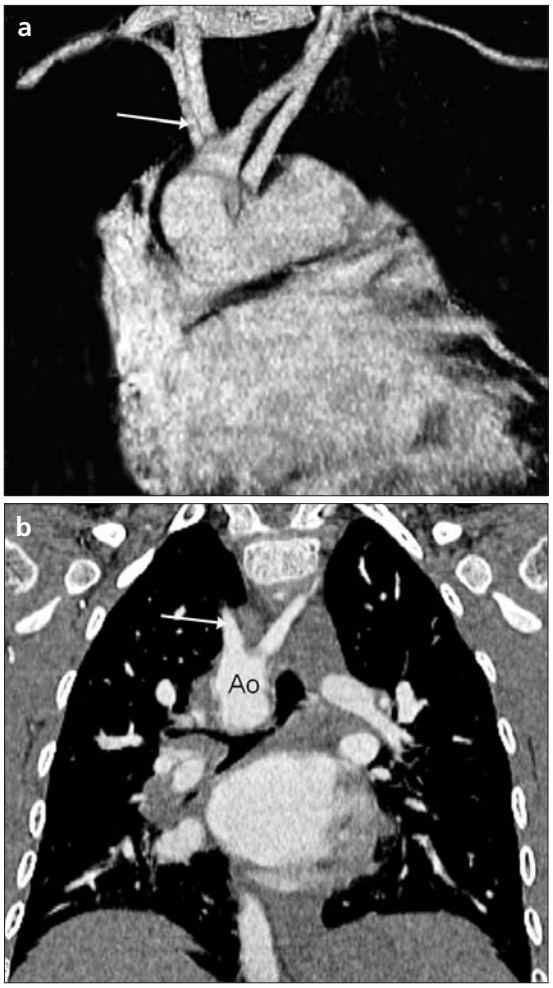

Figure 5. a, b. Aberrant right subclavian artery. On three-dimensional volume rendering CT image **(a)** of a 4-year-old patient, the right subclavian artery is separated from the distal of the aortic arch *(arrow)*. On coronal reformatted CT image **(b)**, the right subclavian artery *(arrow)* is observed to separate after it originates from the left subclavian artery (Ao, aorta).

I. d. Interrupted aortic arch

Interrupted aortic arch malformation comprises 1% of congenital heart defects (11, 17). The disruption between the ascending and descending aorta is known as interrupted aortic arch and is classified according to the state of the interruption (8, 11, 18):

Type A: The interruption is on the distal left subclavian artery (30% of cases).

Type B: The interruption is between the left carotid artery and the left subclavian artery (43% of cases). Aberrant right subclavian artery is common; DiGeorge syndrome has been reported in nearly 50% of the cases.

Type C: The interruption is between the innominate artery and the left carotid arteries (17% of cases).

Each of these types is further divided into subtypes 1: normal subclavian artery; subtype 2: aberrant subclavian artery; subtype 3: isolated subclavian artery originating from the ductus arteriosus (8).

This anomaly is an advanced form of aortic coarctation, characterized by aortic atresia or absence of aortic arch segment. The descending aorta receives its blood supply from a patent ductus arteriosus and systemic collaterals. Despite the definition of the relation between interrupted aortic arch and various congenital heart defects, literature reveals only one case with coexisting absence of the left carotid artery and interrupted aortic arch (18). Echocardiography is not always effective in evaluation of the aortic segment in coarctation. CA effectively shows the anatomical structure, but it is time consuming and invasive. MPR and 3D imaging through multidetector CTA is a noninvasive imaging method that can clearly display the interrupted aortic arch and collateral vessels and the anatomical structures (Fig. 4).

I. e. Aberrant right subclavian artery

The incidence of aberrant right subclavian artery varies between 0.5% and 2% among general population. The aberrant artery usually courses posterior to the esophagus and rarely anterior to the trachea or esophagus and arrives at the right arm. When the right subclavian artery branches off independent of the descending aorta, it courses posterior to the esophagus and compresses it, thus causing vascular circulation problems (15). Aberrant right subclavian artery may be accompanied by anomalies such as non-recurrent right inferior laryngeal nerve, aortic coarctation, interrupted aortic arch, and right-sided aortic arch (19). As an imaging method, esophagography with barium can also show the compression on the posterior of the esophagus. Furthermore, CA, an invasive method, and MDCT angiography, a noninvasive method, can clearly show the aberrant artery (Fig. 5). In the origin of the right subclavian artery, diverticula may be detected as residue of the right dorsal aortic artery root. A diverticulum may develop

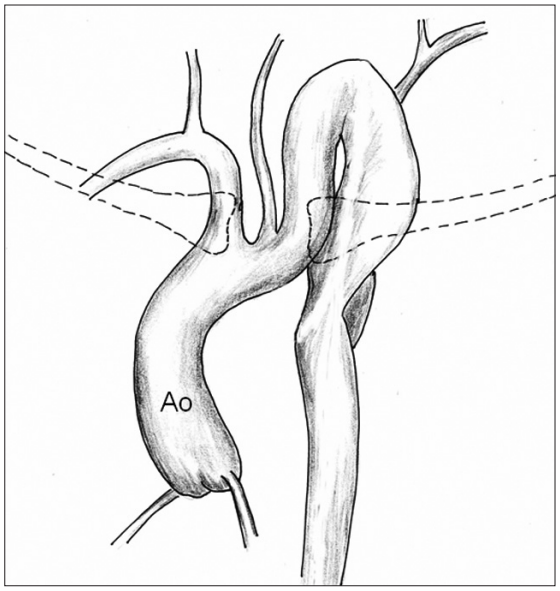

Figure 6. Cervical aortic arch. The aortic arch is observed over the clavicle (Ao, aorta).

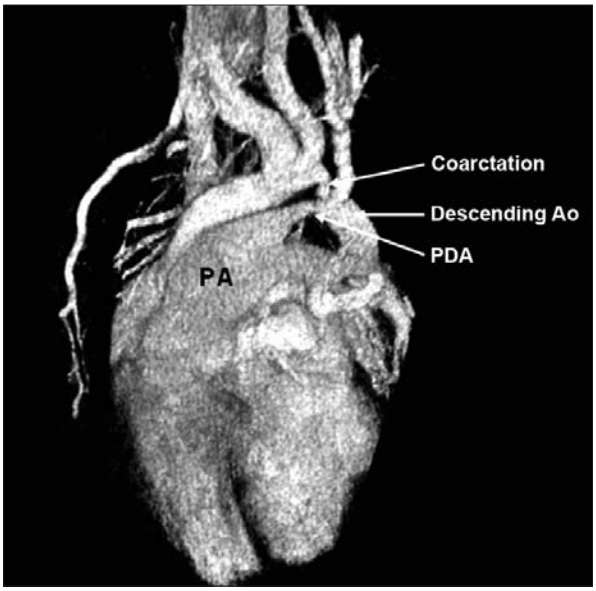

Figure 7. Patent ductus arteriosus and aortic coarctation. On three-dimensional volume rendering CT image of a 6-month-old infant, the ductus is seen between the pulmonary artery and the aorta through an oblique view. At the same time, proximal to the exit of the left subclavian artery, a stenotic segment related to coarctation is seen (Ao, aorta; PA, pulmonary artery; PDA, patent ductus arteriosus).

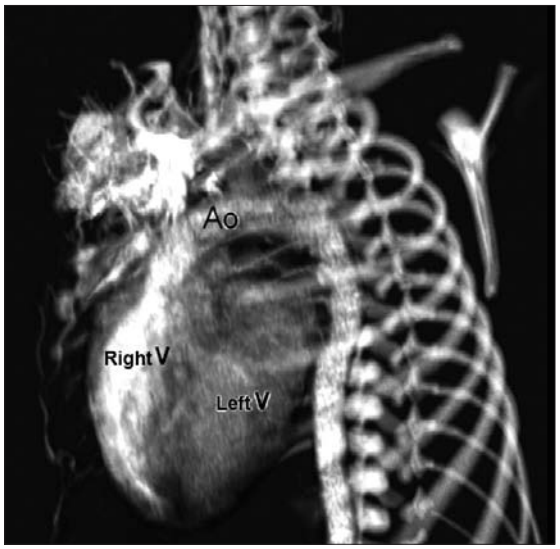

Figure 8. Complete transposition of the great arteries. On three-dimensional volume rendering CT image of a 10-day-old infant, the aorta is observed to be the main vascular structure closest to the front chest wall and exits the right ventricle through a left oblique view (Ao, aorta; V, ventricle).

into an aneurysm with age and be ruptured.

I. f. Cervical aortic arch

Cervical aortic arch is a rare anomaly in which the aortic arch is located over the clavicle and is usually right sided (Fig. 6). CA and MDCT angiography provide accurate diagnosis (11).

I. g. Patent ductus arteriosus

Patent ductus arteriosus (PDA) is the persistent fetal structure between the left pulmonary artery and descending aorta after birth. It is located 5–10 mm distal to the origin of the left subclavian artery (8, 11). The ductus may be short, long, straight, or tortuous. In term infants, PDA comprises 5% to 10% of congenital heart disease, but it is much more common in premature infants (and is twice as common in females as in males) (8, 11). Hemodynamically, there is a shunt between the aorta and the pulmonary artery from the left to the right. Coexisting persistent postnatal hypoxia and maternal rubella play a role in the etiology. Embryologically, the ductus originates from the primitive sixth aortic arch. Imaging methods are chest radiography, echocardiography, and CA. Coronal, sagittal, and 3D images obtained through multidetector CTA provide important information on the location of the ductus and the other anatomical variations (Fig. 7).

I. h. Complete transposition of the great arteries

Transposition of the great arteries (TGA) is the most common cyanotic congenital heart disease seen in the newborn, and it comprises almost 5% of cases of congenital heart disease. In this anomaly, the pulmonary artery originates from the left ventricle, and ascending aorta originates from the right ventricle (8, 20). Survival is not possible without mixing of systemic and pulmonary circulation via one or more sites, most commonly atrial septal defect, ventricular septal defect, and PDA. Males are affected more than females, with a 3:1 ratio (11). It has an incidence of 1 in 3000 live births. Clinically, mild cyanosis that does not improve with oxygen may be observed.

Chest radiography, echocardiography, MR, and CA are imaging methods used in detecting this anomaly. MPR and 3D VR obtained through multidetector CTA show the abnormal ventriculoarterial relation in detail (Fig. 8). Furthermore, the axial section at the

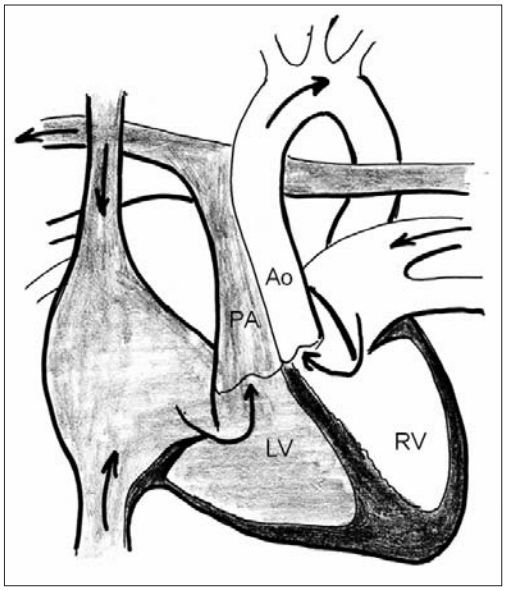

Figure 9. Congenitally corrected transposition. The aorta originates from the morphological right ventricle (located on the left), and the pulmonary artery originates from the morphological left ventricle (located on the right). In addition, the aorta is seen anterior and to the left of the pulmonary artery (Ao, aorta; PA, pulmonary artery; RV, right ventricle; LV, left ventricle).

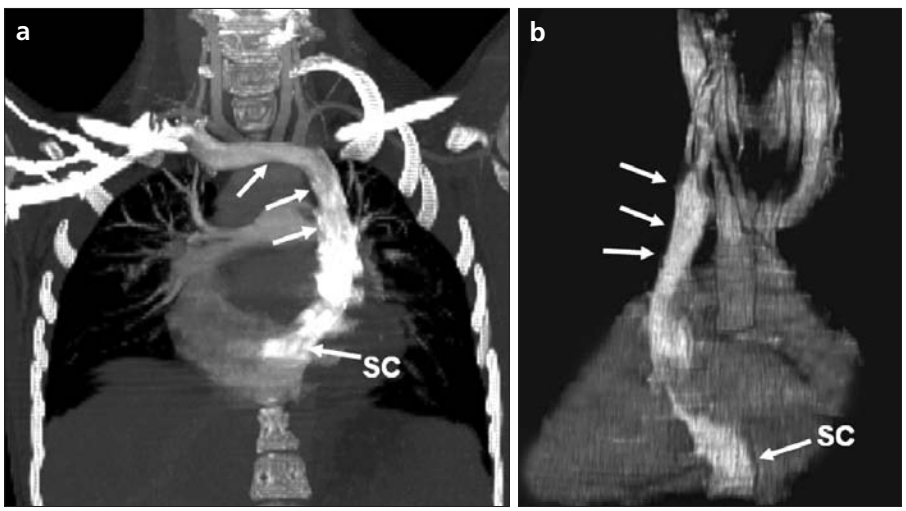

Figure 10. a, b. Persistent left superior vena cava (SVC). On maximum intensity projection **(a)** and three-dimensional volume rendering **(b)** CT images of a 1-year-old patient, the SVC is located on the left *(arrows)* and persists in the right atrium through coronary sinus (SC, sinus coronarius).

aortic root level shows that the aorta is located anteriorly and on the right of the pulmonary artery. On the sagittal images, considering the pulmonary artery, the anterior location of the aorta connecting to the right ventricle can easily be identified.

I. i. Congenitally corrected transposition

There are both ventriculoarterial and atrioventricular discordance in this anomaly, which is defined as inverted ventricles and great arteries (8). The aorta originates from the morphological right ventricle (located on the left), and the pulmonary artery originates from the morphological left ventricle, located on the right. The aorta is located anterior and to the left of the pulmonary artery (Fig. 9). The imaging methods used resemble those used in TGA. Through multidetector CTA, abnormal atrioventricular and ventriculoarterial relationship can be clearly shown.

II. Venous anomalies

Since determination of venous anatomical variants and congenital anomalies is essential in vascular surgery, knowledge of the image characteristics of these anomalies, which may be overlooked, is also essential (21).

II.a. Superior vena cava anomalies

II.a.1. Persistent left superior vena cava

The left superior vena cava (SVC) occurs in 3% to 5% of the patients with congenital heart disease, and 0.3% to 0.5% of the general population (11, 22). Complete regression of the right SVC forms by the development of the left anterior cardinal vein (22). Blood transported by the left SVC most commonly reaches the right atrium through the coronary sinus. This anomaly is usually asymptomatic and does not require treatment unless accompanied by other cardiac anomalies (11, 22, 23). Rarely, the left SVC drains into the left atrium as a result of arterial desaturation (11). The left SVC has been reported to be identifiable in the fetus and be accompanied by coarctation and arch hypoplasia (24). The left SVC opening to the right atrium through the coronary sinus can be clearly shown by MPR and 3D VR obtained through MDCT (Fig. 10).

II.a.2. Double superior vena cava

Double SVC is seen in 0.3% of the general population and 11% of those with congenital heart disease (22). Double SVC leads to clinical symptoms only when the left branch opens to the left atrium. Abnormal convergence of the left superior pulmonary vein with the left vein might mimic double SVC. Convergence with the anonymous vein can be confirmed; on CT, the left superior pulmonary vein is observed at the level of the left pulmonary artery (Fig. 11).

II.a.3. Superior vena cava agenesis and drainage into the inferior vena cava through azygous vein

Total absence of the SVC is extremely rare and is associated with undeveloped right anterior cardinal vein (22). The blood from the upper extremity and the head reaches the right atrium through a venous plexus formed by the azygous vein cranio-caudally coursing below the diaphragm. In this anomaly, the azygous vein usually has a dilated appearance, and blood flow is directed toward the inferior vena cava.

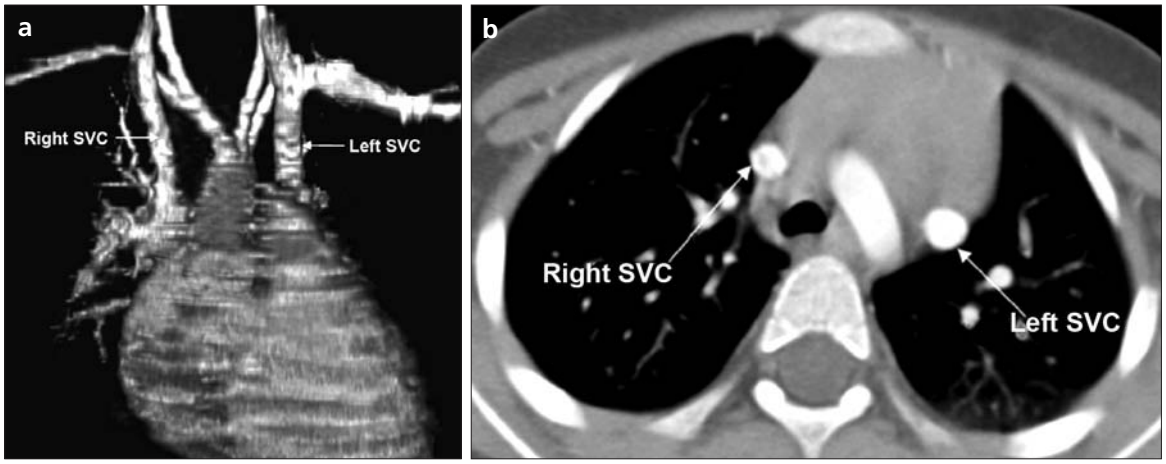

Figure 11. a, b. Double superior vena cava (SVC). On three-dimensional volume rendering CT image **(a)** of a 3-year-old patient, double SVC is observed through an anterior view. On the axial CT section **(b)**, vena cava is seen on each side of the aorta (SVC, superior vena cava).

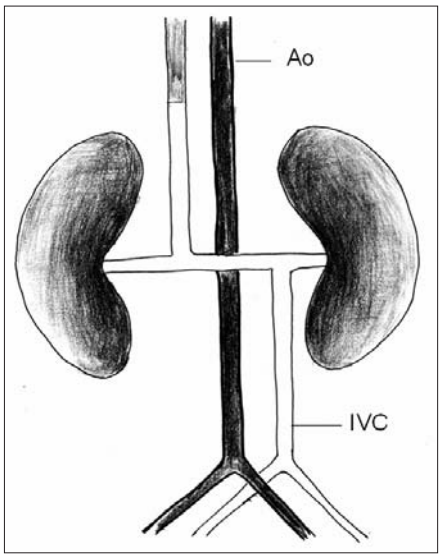

Figure 12. Left inferior vena cava (IVC). The IVC has shifted toward the right in front of the aorta at the level of the renal hilus and formed a mirror image of normal (Ao, aorta, IVC, inferior vena cava).

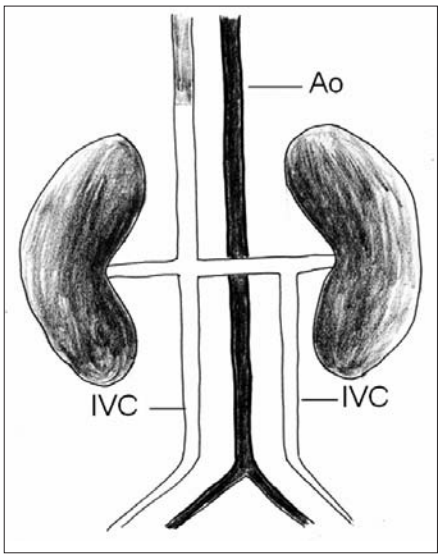

Figure 13. Double inferior vena cava (IVC). At the subrenal level, veins of IVC are observed on both sides of the aorta; these two veins are combined at the renal hilus level, descending as a single right IVC (Ao, aorta, IVC, inferior vena cava).

II.b. Inferior vena cava anomalies

Inferior vena cava (IVC) anomalies are often associated with congenital heart diseases, with a rate of 0.6% to 2% in patients with cardiovascular defects and a rate of 0.3% in those with no defects (25).

II.b.1. Left inferior vena cava

Left inferior vena cava has a prevalence of 0.2% to 0.5% in the general population; embryogenically, it is formed by the regression of the right supracardinal vein and persistent left supracardinal vein. It presents the mirror image of normal structures. The IVC moves to the right anterior of the aorta at the level of the kidney hilus (Fig. 12) (22). The anomaly mimics left-sided paraaortic lymphadenopathy, and may result in an inaccurate diagnosis. Moreover, it may cause difficulties in patients requiring IVC filter (26). Demonstration of these findings on CT is of great importance for surgical procedures.

II.b.2. Double inferior vena cava

The incidence of double IVC is 1% to 3% in the general population. It is formed as a result of the persistence of both supracardinal veins at the subrenal level. At the subrenal level, the IVC is observed on both sides of the aorta; at the level of renal hilus, both veins combine as a single right IVC (Fig. 13); double right IVC has also been identified (22, 27). The size of the left and right veins may be asymmetrical. Double IVC should be suspected in cases with recurrent pulmonary emboli following IVC filters. Like left IVC, it may be mistaken for paraaortic lymphadenopathy (26).

II.b.3. Absence of the subrenal segment of the inferior vena cava

In the absence of the subrenal segment of the IVC, the venous drainage of the lower extremities is provided by sacral, lumbar, and epigastric vein anastomoses. This anomaly is usually not associated with congenital anomalies. Many authors have claimed that this condition occurs during prenatal period or right after birth as a result of thrombosis in the subrenal segment of IVC (Fig. 14) (22).

II.b.4. Inferior vena cava with azygos vein continuation

IVC with azygos vein continuation is rare, with a prevalence of 0.6% of the general population. It has been reported in nearly 3% of the children with congenital heart defect. The IVC is normal below the level of renal vein but has no hepatic segment (11, 22). Because of the agenesis of the hepatic segment of the IVC, the blood circulation in the caudal segment reaches the azygous vein system through persistent right supracardinal vein (22). The IVC drains into the SVC and eventually into the right atrium through the enlarged azygous vein system. The hepatic veins are directly connected to

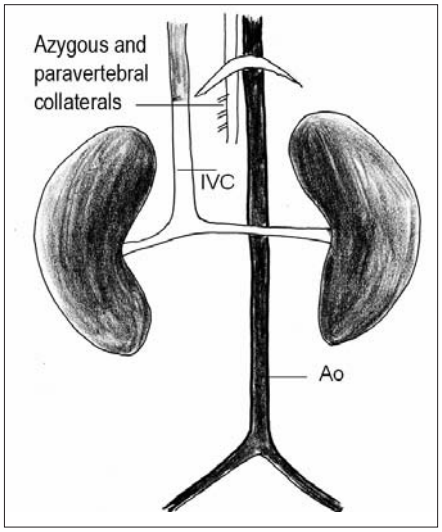

Figure 14. Absence of the subrenal segment of the inferior vena cava (IVC). At the subrenal level, the absence of IVC is observed (Ao, aorta, IVC, inferior vena cava).

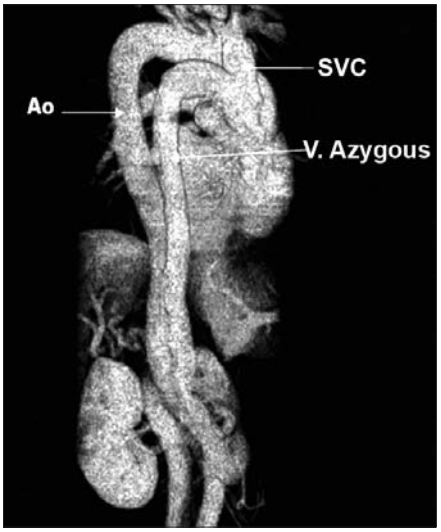

Figure 15. Drainage of the inferior vena cava (IVC) through azygous vein. On three-dimensional volume rendering CT image of a 54-year-old patient, the IVC drains into the superior vena cava through azygous vein on posterior view *(arrows)* (Ao, aorta, SVC, superior vena cava).

the right atrium (11). The relationship of IVC with azygous vein may coexist with complex cyanotic heart disease, polysplenia syndrome, the right ventricle with double exit, pulmonary venous backflow anomalies, and absence of the minor fissure of the right lung (11, 22, 28). Direct relationship of the IVC with the left atrium is rare. In such a case, the IVC receives the hepatic veins and directly connects with the left atrium (11). To avoid misdiagnoses, the recognition of enlarged azygous vein in these areas is important. A thorough knowledge of the anatomy is essential in planning cardiac surgery and catheterization procedures (26). The relationship of the azygous vein with IVC and the atria can be clearly demonstrated by MPR and 3D VR images obtained through MDCT, which will provide important information for the surgeon (Fig. 15).

In conclusion, MDCT provides reliable diagnostic information on the normal anatomy of the aorta and vena cava, as well as congenital anomalies in pediatric and adult patients. Despite offering diagnostic information for evaluation of these vascular anomalies, axial images remain ineffective in diagnosis of small coarctation and shunt lesions. In anomalies of this kind, MPR and 3D VR images have increased the diagnostic value of CT (5, 12). Furthermore, coronal and sagittal views of the aorta facilitate the orientation of a surgeon, and thus aid in planning surgery. As primary cardiac imaging methods, echocardiography and CA are widely used. However, echocardiography has disadvantages such as showing a small area, operator dependency, and limited capability in defining extracardiac structures (8); and CA requires prolonged sedation and produces catheter-related complications. In addition, the great vessels and their branches overlap each other on CA and make the identification of each difficult (5, 8, 12).

MRA does not contain ionized radiation and can be performed without contrast media. However, it is time consuming, requires prolonged sedation, and creates difficulties in imaging of the patients with severe illness or inability to cooperate (5, 8). With its volumetric imaging quality, multidetector CTA clearly demonstrates the aorta, vena cava, and pulmonary artery and their branches. Moreover, it requires shorter imaging time and shorter sedation. It is also a noninvasive method, providing a scanning chance for patients that cannot tolerate MRI. CTA has a radiation risk; however, in severely ill patients, prolonged sedation risk is more critical than radiation damage, and thus CTA is preferred because of its fast imaging quality at a low dose. We believe that because of these advantages, use of multidetector CTA in the evaluation of vascular pathologies will continue to increase in importance.

References

1. Gravereaux EC, Nguyen LL, Cunningham LD. Congenital vascular anomalies. Curr Treat Options Cardiovasc Med 2004; 6:129–138.
2. Prokop M. Multislice CT angiography. Eur J Radiol 2000; 36:86–96.
3. Akin O, Coşkun M. Multi-detector CT angiography: technique and clinical applications. Tani Girisim Radyol 2003; 9:139–145.
4. Gilkeson RC, Ciancibello L, Zahka K. Pictorial essay. Multidetector CT evaluation of congenital heart disease in pediatric and adult patients. AJR Am J Roentgenol 2003; 180:973–980.
5. Lee EY, Siegel MJ, Hildebolt CF, Gutierrez FR, Bhalla S, Fallah JH. MDCT evaluation of thoracic aortic anomalies in pediatric patients and young adults: comparison of axial, multiplanar, and 3D images. AJR Am J Roentgenol 2004; 182:777–784.
6. Kalra MK, Maher MM, D'Souza R, Saini S. Multidetector computed tomography technology: current status and emerging developments. J Comput Assist Tomogr 2004; 28(Suppl 1):S2–S6.
7. Oguz B, Haliloglu M, Karcaaltincaba M. Paediatric multidetector CT angiography: spectrum of congenital thoracic vascular anomalies. Br J Radiol 2006; 80:376–383.
8. Goo HW, Park IS, Ko JK, et al. CT of congenital heart disease: normal anatomy and typical pathologic conditions. Radiographics 2003; 23:147–165.
9. Lindsay J Jr. Coarctation of the aorta, bicuspid aortic valve and abnormal ascending aortic wall. Am J Cardiol 1988; 61:182–184.
10. Schertler T, Wildermuth S, Boehm T. Coarctation and aorto-aortic bypass: three-dimensional post-processing using multidetector row computed tomography. Heart Vessels 2005; 20:88–90.
11. Park MK. Pediatric cardiology for practitioners. 4th ed. St. Louis: Mosby, 2002:141–263.
12. Siegel MJ. Multiplanar and three-dimensional multi-detector row CT of thoracic vessels and airways in the pediatric population. Radiology 2003; 229:641–650.
13. Fleck RJ, Pacharn P, Fricke BL, Ziegler MA, Cotton RT, Donnelly LF. Imaging findings in pediatric patients with persistent airway symptoms after surgery for double aortic arch. AJR Am J Roentgenol 2002; 178:1275–1279.
14. Dicenta F, Rodriguez JA, Belloch V. Double aortic arch. Rev Esp Cardiol 2002; 55:1088.
15. Alper F, Akgun M, Kantarci M, et al. Demonstration of vascular abnormalities compressing esophagus by MDCT: special focus on dysphagia lusoria. Eur J Radiol 2006; 59:82–87.
16. Bonnard A, Auber F, Fourcade L, Marchac V, Emond S, Revillon Y. Vascular ring abnormalities: a retrospective study of 62 cases. J Pediatr Surg 2003; 38:539–543.

17. Cinar A, Haliloglu M, Karagoz T, Karcaaltincaba M, Celiker A, Tekinalp G. Interrupted aortic arch in a neonate: multidetector CT diagnosis. Pediatr Radiol 2004; 34:901–903.
18. Onbas O, Olgun H, Ceviz N, Ors R, Okur A. Interrupted aortic arch associated with absence of left common carotid artery: imaging with MDCT. Cardiovasc Intervent Radiol 2006; 29:429–431.
19. Ebstein DA, Debort JR. Abnormalities associated with aberrant right subclavian arteries: a case report. Vasc Endovascular Surg 2002; 36:297–303.
20. Kawano T, Ishii M, Takagi J, et al. Three dimensional helical computed tomographic angiography in neonates and infants with complex heart disease. Am Heart J 2000; 139:654–660.
21. Gomes MN, Choyke PL. Assessment of major venous anomalies by computerized tomography. J Cardiovasc Surg 1990; 31:621–628.
22. Minniti S, Visentini S, Procacci C. Congenital anomalies of the venae cavae: embryological origin, imaging features and report of three new variants. Eur Radiol 2002; 12:2040–2055.
23. Gerber TC, Kuzo RS. Images in cardiovascular medicine. Persistent left superior vena cava demonstrated with multislice spiral computed tomography. Circulation 2002; 105:79.
24. Pasquini L, Fichera A, Tan T, Ho SY, Gardiner H. Left superior caval vein: a powerful indicator of fetal coarctation. Heart 2005; 91:539–540.
25. Gayer G, Zissin R, Strauss S, Hertz M. IVC anomalies and right renal aplasia detected on CT: a possible link? Abdom Imaging 2003; 28:395–399.
26. Bass JE, Redwine MD, Kramer LA, Huynh PT, Harris JH Jr. Spectrum of congenital anomalies of the inferior vena cava: cross-sectional imaging findings. Radiographics 2000; 20:639–652.
27. Mathews R, Smith PA, Fishman EK, Marshall FF. Anomalies of the inferior vena cava and renal veins: embryologic and surgical considerations. Urology 1999; 53:873–880.
28. Roguin N, Hammerman H, Korman S, Riss E. Angiography of azygos continuation of inferior vena cava in situs ambiguus with left isomerism (polysplenia syndrome). Pediatr Radiol 1984; 14:109–112.